International Journal of Theoretical Physics, Vol. 22, No. 11, 1983

Production of Charged Multileptons in $\bar{p}p$ Collisions

G. C. Chukwumah

Department of Mathematics, University of Nigeria, Nsukka, Nigeria

Received May 15, 1981

With the prospects for the $\bar{p}p$ colliding beam experiments in view, with the center-of-mass energy $\sqrt{s}$ in the range 20–800 GeV, it is attractive to estimate the contribution of heavy particle pairs to charged multilepton production. In this paper we estimate cross sections of charged multilepton yields from the weak, semileptonic, and cascade decays of the bottom and top particle pairs produced in inclusive $\bar{p}p$ collisions. Such cross sections may serve as additional inputs in any future experimental searches for the top flavor. They may also help to discriminate quark mixing angles when precise charged multilepton signals become available.

1. INTRODUCTION

According to the present theoretical picture, t decays may occur sequentially through the chain

$$t \searrow b.... \searrow c.... \searrow s.... \tag{1}$$

Each step in the cascade decay chain of the heavy quarks: charm, bottom, and top, is associated with a probability for emitting a charged lepton. The probability for identifying one or more charged leptons among the overall

0020-7748/83/1100-0997$03.00/0

decay products of heavy particle pairs may be a possible signature for identifying the production of new flavors. Taking into consideration the projected $\bar{p}p$ colliding beam experiments with the center-of-mass energy, $\sqrt{s}$ as large as 800 GeV, one would settle for the production of the heavy particle pairs, specifically the top and bottom pairs, in inclusive $\bar{p}p$ collisions.

In calculating the particle-pair cross sections, we follow the structure of the parton model. In which case, the production of the bottom and top quarks occurs through the interaction of light quarks and gluons. In the production of $b\bar{b}$ and $t\bar{t}$ pairs in $\bar{p}p$ collisions the contributing subprocesses considered are the following:

$$q\bar{q} \to h\bar{h} \tag{2}$$

and

$$gg \to h\bar{h} \tag{3}$$

where q denotes a light quark (u, d, s), g a vector gluon, and h the bottom quark b, or the top quark, t. Equations (2) and (3) are the flavor-creating subprocesses. One of our basic assumptions is that an $h\bar{h}$ pair produced via the subprocesses will usually evolve into a pair of naked bottom or top state if $m_{h\bar{h}}$ is above the appropriate threshold mass.

Thus,

$$\sigma(\bar{p}p \to b \text{ or } t \text{ particle pairs} + X) \approx \sigma(\bar{p}p \to h\bar{h} + X, m_{h\bar{h}} > 2m_H) \tag{4}$$

whereby the threshold invariant mass is taken to be $2m_H$, m_H being the mass of the lowest-lying h state. We also assume that no other flavor of quark may dress to form a bottom or top hadron state, so that the outgoing bottom or top quarks are dressed to form bottom and top hadrons with a unit probability, independent of their momenta.

The rest of the paper is organized as follows: In Section 2, we give the production formalisms and derive expressions for the total cross sections for the production of b and t particle pairs in $\bar{p}p$ collisions, via the subprocesses of equations (2) and (3).

Section 3 deals with the semileptonic decays of the heavy quarks. Here we compute the probabilities of the emission of charged leptons, $e^{\pm}$, $\mu^{\pm}$, in the decay products of the $b\bar{b}$ and $t\bar{t}$ pairs.

In Section 4, we obtain expressions and numerical results for the total cross sections of charged multilepton production from the $b\bar{b}$ and $t\bar{t}$ decays.

In Section 5, we present our summary.

2. FORMALISM OF b AND t PARTICLE PAIR PRODUCTION IN $\bar{p}p$ INTERACTION

We recall the contributing subprocesses to $b\bar{b}$ and $t\bar{t}$ pair production, in $\bar{p}p$ interaction, namely,

$$q\bar{q} \to h\bar{h}X \qquad \text{and} \qquad gg \to h\bar{h}X$$

where $h = (b \text{ or } t)$.

The Feynman diagrams for the subprocesses are as shown in Figures 1 and 2, respectively.

The matrix element for $q\bar{q} \to h\bar{h}X$ is given by

$$M = -\frac{\delta_{\alpha\beta} g^2}{(p_h + p_{\bar{h}})^2} T^b_{ik} T^b_{lj} \bar{u}(p_h) \gamma_\mu v(p_{\bar{h}}) \bar{v}(p_2) \gamma_\mu u(p_1), \tag{5}$$

where i, j, k, l are the quark color indices; $\alpha = u, d, s$, $\beta = \bar{u}, \bar{d}, \bar{s}$; a, b, c are the gluon color indices and $T^a = \lambda^a/2$, etc., where the λ's are the well-known Gell-Mann $SU(3)$ generators of color.

Squaring (5), averaging over initial color degrees of freedom, and taking the traces, we obtain

$$|\overline{M}|^2 = \frac{256}{9} \frac{\pi^2 \alpha_s^2(Q^2)}{m_\alpha^2 m_h^2 \hat{S}^2} \left[(p_1 \cdot p_{\bar{h}})(p_2 \cdot p_h) + m_h^2 (p_1 \cdot p_2) + m_\alpha^2 (p_h \cdot p_{\bar{h}}) \right.$$

$$\left. + (p_1 \cdot p_h)(p_2 \cdot p_{\bar{h}}) + 2 m_\alpha^2 m_h^2 \right] \tag{6}$$

where m_α is the mass of a light quark, q. Naively, we have taken $m_u = m_d = m_s = m_\alpha$. Introducing the Mendelstam invariants, $\hat{u}, \hat{s}, \hat{t}$, with $\hat{s} + \hat{t} + \hat{u} = 2m_h^2$, we obtain

$$p_1 \cdot p_h = p_2 \cdot p_{\bar{h}} = \tfrac{1}{2}\left(m_h^2 + m_\alpha^2 - \hat{t}\right)$$

$$p_1 \cdot p_{\bar{h}} = p_h \cdot p_2 = \tfrac{1}{2}\left(m_h^2 + m_\alpha^2 - \hat{u}\right)$$

and

$$p_1 \cdot p_2 = p_h \cdot p_{\bar{h}} = \hat{s}/2 - m_\alpha^2 \tag{7}$$

so that equation (6) gives

$$|\overline{M}|^2 = \frac{64}{9} \frac{\pi^2 \alpha_s^2(Q^2)}{m_\alpha^2 m_h^2} \cdot \frac{1}{\hat{s}^2} \left(2m_h^4 + 4m_h^2 \hat{s} - 4m_h^2 \hat{t} + \hat{s}^2 + 2\hat{s}\hat{t} + 2\hat{t}^2\right) \tag{8}$$

The total cross section for the subprocess is given by the hard scattering relation:

$$\sigma^{q\bar{q} \to h\bar{h}}(\hat{s}) = \frac{1}{16\pi \hat{s}^2} \int_{t_{\min}}^{t_{\max}} |\overline{M}|^2 \, dt \tag{9}$$

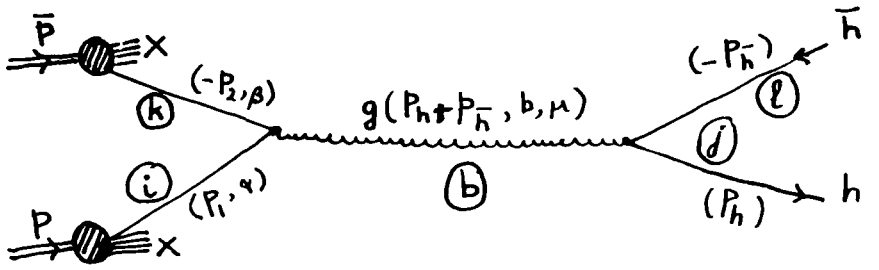

Fig. 1. Lowest-order Feyman diagram for $q\bar{q} \to h\bar{h}X$ contributing to top (t) and beauty (b) production in $\bar{p}p$ collisions.

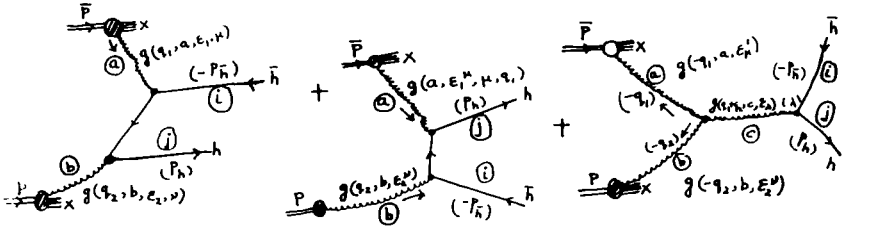

Fig. 2. Lowest-order Feyman diagrams for $gg \to h\bar{h}X$.

where

$$t_{\max}(t_{\min}) = m_h^2 - \frac{\hat{s}}{2} \pm \tfrac{1}{2}\left[\hat{s}\left(\hat{s} - 4m_h^2\right)\right]^{1/2} \tag{10}$$

Substituting (8) into (10), one obtains

$$\overset{q\bar{q} \to h\bar{h}}{\sigma}(\hat{s}) = \frac{8\pi}{27}\frac{\alpha^2(Q^2)}{m_a^2 m_h^2}\frac{\left[\hat{s}\left(\hat{s} - 4m_h^2\right)\right]^{1/2}}{\hat{s}^3}\left(2m_h^2 + \hat{s}\right) \tag{11}$$

The contribution of the subprocess to the total cross section is

$$\begin{aligned}\left(\sigma\left(\bar{p}p \to h\bar{h}X\right)\right)_{\text{total}} &= \overset{q\bar{q} \to h\bar{h}}{\int_{4m_h^2/s}^{1}} dx\, u_v^p(x, Q^2)\, X \\ &\quad \times \int_{4m_h^2/sx}^{1} dy \cdot u_v^p(y, Q^2) \cdot \sigma_{(xys)}^{q\bar{q} \to h\bar{h}} \\ &\quad + \int_{4m_h^2/s}^{1} d_v^p(x, Q^2) \int_{4m_h^2/sx}^{1} dy\, d_v^p(y, Q^2)\, \sigma_{(xys)}^{q\bar{q} \to h\bar{h}}\end{aligned} \tag{12}$$

where $\hat{s} = xys$ and s is the antiproton–proton center-of-mass energy squared. We note that there are no valence antiquarks inside the proton.

Next, we consider the subprocesses

$$gg \to h\bar{h}$$

whose Feynman diagrams are in Figure 2. The matrix element is given by

$$\begin{aligned} M = {} & g^2 \bar{u}(p_h) T^a T^b \gamma_\nu \varepsilon_2^\nu \left[\frac{(\not{q}_1 - \not{p}_{\bar{h}} + m_h)}{(q_1 - p_{\bar{h}})^2 - m_h^2} \gamma_\mu \varepsilon_1^\mu \right] \\ & + T^b T^a \gamma_\mu \varepsilon_1^\mu \left[\frac{(\not{q}_2 - \not{p}_{\bar{h}}) \gamma_\nu \varepsilon_2^\nu}{(q_2 - p_{\bar{h}})^2 - m_h^2} \right] \\ & + i f^{abc} G^{\mu\nu\lambda}(-q_1, -q_2, q_1 + q_2) \frac{\varepsilon^\mu \varepsilon_2^\nu \gamma_\lambda T^c}{(q_1 + q_2)^2} v(p_{\bar{h}}) \end{aligned} \tag{13}$$

where $G^{\mu\nu\lambda}$ is a tensor connected with the three-gluon vertex. Expanding $G^{\mu\nu\lambda}$, we obtain

$$\begin{aligned} G^{\mu\nu\lambda}(-q_1, -q_2, q_1 + q_2) = {} & (q_2 - q_1)^\lambda g_{\mu\nu} + (-2q_2 - q_1)^\mu g_{\nu\lambda} \\ & + (2q_1 + q_2)^\nu g_{\lambda\mu} \end{aligned}$$

so that equation (13) gives, for transverse gluons only,

$$\begin{aligned} |\overline{M}|^2 = {} & \frac{g^4}{4(\hat{t} - m_h^2)^2} \operatorname{Tr}(T^a T^b T^b T^a) \\ & \times \operatorname{Tr}\{\gamma_\nu (\not{q}_1 - \not{p}_{\bar{h}} + m_h) \gamma_\mu [-\Lambda^-(p_{\bar{h}})] \gamma_\mu (\not{q}_1 - \not{p}_h + m_h)\} \\ & + \frac{g^4}{(\hat{u} - m_h^2)^2} \operatorname{Tr}(T^b T^a T^a T^b) \\ & \times \operatorname{Tr}[\gamma_\mu (\not{q}_2 - \not{p}_{\bar{h}} + m_h) \gamma_\nu [-\Lambda^-(p_{\bar{h}})] \gamma_\nu (\not{q}_2 - \not{p}_{\bar{h}} + m_h) \gamma_\mu \Lambda(p_h)] \\ & + \frac{g^4}{4\hat{s}^2} \cdot \operatorname{Tr}[i f^{abc} f^{abc} G^{\mu\nu\lambda} \gamma_\lambda T^c T^{c*} [-\Lambda^-(p_{\bar{h}})] \gamma_\lambda \Lambda(p_h)] \\ & + \frac{g^4}{4(\hat{t} - m_h^2)(\hat{u} - m_h^2)} \operatorname{Tr}(T^a T^b T^a T^b) \\ & \times \operatorname{Tr}\{\gamma_\nu (\not{q}_1 - \not{p}_{\bar{h}} + m_h) \gamma_\mu [-\Lambda^-(p_{\bar{h}})] \gamma_\nu (\not{q}_2 + \not{p}_{\bar{h}} + m_h)\} \end{aligned}$$

$$\times \mathrm{Tr}\{\gamma_\nu(\not q_1 - \not p_{\bar h} + m_h)\gamma_\mu[-\Lambda^-(p_{\bar h})]\gamma_\nu(\not q_2 + \not p_{\bar h} + m_h)\gamma_\mu \Lambda(p_h)\}$$

$$+ \frac{g^4}{4(\hat t - m_h^2)(\hat u - m_h^2)}\left\langle -\frac{1}{96}\right\rangle$$

$$\times \mathrm{Tr}\{\gamma_\mu(\not q_2 \not p_{\bar h} + m_h)\gamma_\nu[-\Lambda^-(p_{\bar h})]\gamma_\mu(\not q_1 - \not p_h + m_h)\gamma_\nu \Lambda(p_h)\}$$

$$+ \frac{g^4}{4s(\hat t - m_h^2)}\left\langle \frac{3}{32}\right\rangle \mathrm{Tr}\{\gamma_\nu(\not q_1 - \not p_{\bar h} + m_h)\gamma_\mu[-\Lambda^-(p_{\bar h})]$$

$$\times \gamma_\lambda G^{\mu\nu\lambda}\Lambda(p_h)\} + \frac{g^4}{4\hat s(\hat t - m_h^2)}\left\langle \frac{3}{32}\right\rangle$$

$$\times \mathrm{Tr}\{G^{\mu\nu\lambda}\gamma_\lambda[-\Lambda^-(p_{\bar h})]\gamma_\mu(\not q_1 - \not p_{\bar h} + m_h)\gamma_\nu \Lambda(p_h)\}$$

$$+ \frac{g^4}{4\hat s(\hat u - m_h^2)}\left\langle \frac{-3}{32}\right\rangle \mathrm{Tr}\{\gamma_\mu(\not q_2 - \not p_{\bar h} + m_h)\gamma_\nu$$

$$\times [-\Lambda^-(p_{\bar h})]\gamma_\nu G^{\mu\nu\lambda}\Lambda(p_h)\}$$

$$+ \frac{g^4}{4\hat s(\hat u - m_h^2)}\left\langle \frac{-3}{32}\right\rangle \mathrm{Tr}\{G^{\mu\nu\lambda}\gamma_\lambda[-\Lambda^-(p_{\bar h})]\gamma_\nu$$

$$\times (\not q_2 - \not p_{\bar h} + m_h)\gamma_\mu \Lambda(p_h)\} \tag{14}$$

Introduce $\hat s, \hat t, \hat u$, with $\hat u + \hat t + \hat s = 2m_h^2$, to obtain the following:

$$q_1 \cdot q_2 = \frac{\hat s}{2}, \qquad p_h \cdot p_{\bar h} = \frac{\hat s}{2} - m_h^2$$

$$q_1 \cdot p_{\bar h} = p_h \cdot p_2 = \frac{m_h^2 - \hat t}{2}$$

$$q_2 \cdot p_{\bar h} = p_h \cdot p_1 = \tfrac{1}{2}(m_h^2 - \hat u) \tag{15}$$

Substitute (15) into (14), to obtain

$$|\overline{M}|^2 = \frac{g^4}{4m_h^2}\left(\frac{1}{12(\hat t - m_h^2)^2}[-14m_h^4 + (8\hat u + 6\hat s)m_h^2 - 2\hat u(\hat u + \hat s)] + \frac{1}{12(\hat u - m_h^2)^2}\right.$$

$$\left. \times [-6m_h^4 + 2m_h^2\hat s - 2\hat u(\hat u + \hat s)] + \frac{3}{16}\cdot\frac{1}{\hat s^2}\right.$$

$$\times\{-4m_h^4+(8\hat{u}-4\hat{s})m_h^2-4[\hat{s}^2+\hat{u}(\hat{u}+\hat{s})]\}$$
$$-\frac{1}{96(\hat{t}-m_h^2)(\hat{u}-m_h^2)}(-16m_h^4+4m_h^2\hat{s})$$
$$-\frac{3}{32}\cdot\frac{1}{(\hat{u}-m_h^2)\hat{s}}(4m_h^4-8m_h^2\hat{u}+4m_h^2\hat{s}+4\hat{u}^2)$$
$$+\frac{3}{32}\cdot\frac{1}{(t-m_h^2)\hat{s}}(-4m_h^4+8m_h^2\hat{u}+4m_h^2\hat{s}-4\hat{u}^2-4\hat{s}^2-8\hat{u}\hat{s})\Bigg) \quad (16)$$

The cross section of the subprocess then gives

$$\overset{gg\to h\bar{h}}{\sigma}(xys)=\frac{\pi\alpha_s^2(Q^2)}{4m_h^2}\Bigg\{\Bigg[\frac{1}{12}-16m_h^2[xys(xys-4m_h^2)]^{1/2}$$
$$-4\frac{[xys(xys-4m_h^2)]^{1/2}}{(xys)^2}-\frac{(4m_h^2+2xys)}{(xys)^2}$$
$$\times\ln\left\{\frac{xys}{2m_h^2}-1-\frac{[xys(xys-4m_h^2)]^{1/2}}{2m_h^2}\right\}$$
$$+\frac{(4m_h^2+2xys)}{(xys)^2}\ln\left\{\frac{xys}{2m_h^2}-1+\frac{[xys(xys-4m_h^2)]^{1/2}}{2m_h^2}\right\}$$
$$+\frac{3}{16(xys)^4}\Bigg\{[xys(xys-4m_h^2)]^{1/2}\Bigg(12m_h^4-\frac{5}{3}xys\cdot m_h^2$$
$$-\frac{35}{6}(xys)^2\Bigg\}+\frac{1}{12}\Bigg(\frac{4m_h^4-m_h^2xys}{(xys)^3}$$
$$\times\ln\left\{\frac{xys}{2m_h^2}-1+\frac{[xys(xys-4m_h^2)]^{1/2}}{2m_h^2}\right\}\Bigg)$$
$$+\frac{3}{8}\Bigg(\frac{2m_h^2}{(xys)^2}\ln\left\{\frac{xys}{2m_h^2}-1+\frac{[xys(xys-4m_h^2)]^{1/2}}{2m_h^2}\right.$$
$$\left.+\frac{[xys(xys-4m_h^2)]^{1/2}}{(xys)^2}\right\}\Bigg)\Bigg\} \quad (17)$$

where $g^2=4\pi\alpha_s(Q^2)$.

The contribution of the subprocess to the $h\bar{h}$ pair production cross section in $\bar{p}p$ collision is

$$\sigma(\bar{p}p \to h\bar{h}X) = \int_{4m^2h/s}^{1} G^p(x,Q^2)\,dx \int_{4m^2h/sx}^{1} G^p(y,Q^2)\,dy\,\sigma^{gg\to h\bar{h}}(xys) \tag{17'}$$

Combine equations (12) and (17') to obtain

$$\begin{aligned}\sigma(\bar{p}p \to h\bar{h}X) = {} & \int_{4m_h^2/s}^{1} u_v^p(x,Q^2)\,dx \int_{4m^2h/sx}^{1} u_v^p(y,Q^2)\,\sigma^{q\bar{q}\to h\bar{h}}(xys) \\ & + \int_{4m_h^2/s}^{1} d_v^p(x,Q^2)\,dx \int_{4m_h^2/sx}^{1} dy\,d_v^p(y,Q^2)\,\sigma^{q\bar{q}\to h\bar{h}}(xys) \\ & + \int_{4m_h^2/s}^{1} G^p(x,Q^2)\,dx \int_{4m_h^2/sx}^{1} G^p(y,Q^2)\,dy \end{aligned} \tag{18}$$

3. SEMILEPTONIC CASCADE DECAYS OF t, b, c, AND CHARGED MULTILEPTON EMISSION FROM DECAY PRODUCTS OF $h\bar{h}$ PAIRS

According to the present theoretical picture, t decays may occur through the chain

$$\begin{array}{l} t \\ \quad \searrow \\ \quad\quad b\ldots \\ \quad\quad\quad \searrow \\ \quad\quad\quad\quad c\ldots. \\ \quad\quad\quad\quad\quad \searrow \\ \quad\quad\quad\quad\quad\quad s\ldots\ldots \end{array} \tag{19}$$

The decay rates for bottom and top, estimated by Cabibbo and Maiani (1979) for each decay channel α, are provided in Tables I and II, respectively. Following a specified parametrization (Maiani, 1977) the quark mixing angles θ, β, γ are bounded as follows (Gaillard and Maiani, 1979):

$$0 \lesssim \beta \lesssim \cdot 5\theta \simeq 0.12, \qquad -0.4 \lesssim \sin\gamma \leqslant 0 \tag{20}$$

The branching ratios of b and t are given by

$$B_r(b \to \alpha) = \frac{\Gamma^b(b \to \alpha)}{\Gamma^b_{\text{total}}(b \to \text{all})} \tag{21}$$

Table I. b Decay Rates in Units of $\Gamma_0^b = G_F^2 m_b^5/193\pi^3$

Channel α	Decay rate (Γ^b/Γ_0^b)
$b \to cl^- \bar{\nu}_l$	$0.41 S_\gamma^2 C_\beta^2$
$\to C\tau^- \bar{\nu}_\tau$	$0.08 S_\gamma^2 C_\beta^2$
$\to ul^- \bar{\nu}_l$	S_β^2
$\to u\tau^- \bar{\nu}_\tau$	$0.39 S_\beta^2$
$\to c\bar{u}d_c$	$1.6 S_\gamma^2 C_\beta^4$
$\to c\bar{c}S_c$	$0.25 C_\gamma^2 S_\gamma^2 C_\beta^2$
$\to u\bar{u}d_c$	$3.9 S_\beta^2 C_\beta^2$
$\to u\bar{c}S_c$	$1.4 S_\beta^2 C_\gamma^2$

with $c\beta = \cos\beta$, etc.; $l^\pm = (\mu^\pm, e^\pm)$.

Table II. t Decay Rates.

t channel α	X_α	g_α(at $m_t \sim 15$ GeV
$t \to bl^+ \nu$	$C_\beta^2 C_\gamma^2$	0.45
$\to b\tau^+ \nu_\tau$	$C_\beta^2 C_\gamma^2$	0.38
$\to ql^+ \nu_l$	$S_\gamma^2 + C_\gamma^2 S_\beta^2$	1.00
$\to q\tau^+ \nu_\tau$	$S_\gamma^2 + C_\gamma^2 S_\beta^2$	0.89
$\to bu\bar{q}$	$3C_\gamma^2 C_\beta^4$	0.45
$\to bc\bar{q}$	$3C_\gamma^2 C_\beta^2 + (C_\gamma^2 + S_\gamma^2 C_\beta^2)$	0.37
$\to qu\bar{q}$	$3C_\beta^2 (S_\gamma^2 + C_\gamma^2 S_\beta^2)$	1.00
$\to qc\bar{q}$	$3(C_\gamma^2 + S_\gamma^2 S_\beta^2)(S_\gamma^2 + C_\gamma^2 S_\beta^2)$	0.88
$\to q\bar{b}c$	$3S_\gamma^2 C_\beta^2 (S_\gamma^2 + C_\gamma^2 S_\beta^2)$	0.38
$\to q\bar{b}u$	$3S_\beta^2 (S_\gamma^2 + C_\gamma^2 S_\beta^2)$	0.45
$\to b\bar{b}c$	$3C_\gamma^2 S_\gamma^2 C_\beta^4$	0.08
$\to b\bar{b}u$	$3C_\gamma^2 C_\beta^2 S_\beta^2$	0.12

where q is a light quark, u, d, s.

and

$$B_r(t \to \alpha) = \frac{\Gamma'(t \to \alpha)}{\Gamma'_{\text{total}}(t \to \text{all})}$$

$$= \Gamma'_0 X_\alpha g_\alpha \Big/ \sum_\alpha \Gamma'_0 X_\alpha g_\alpha$$

$$= X_\alpha g_\alpha \Big/ \sum_\alpha X_\alpha g_\alpha \tag{22}$$

where X_α is the weak coupling factor and g_α is the phase space correction.

Computations of Γ^b_{total} and Γ^t_{total} give

$$\Gamma^b_{\text{total}} \Gamma^b_0 \left(2.75 S_\gamma^2 + 7.69 S_\beta^2 - 5.75 S_\beta^2 S_\gamma^2 - 0.25 S_\gamma^4\right) = \Gamma_0^b R \tag{23}$$

where

$$R = 2.75 S_\gamma^2 + 7.69 S_\beta^2 - 5.75 S_\beta^2 S_\gamma^2 - 0.25 S_\gamma^4 \tag{24}$$

and $S_\gamma = \sin_\gamma$, etc., and

$$\Gamma'_{\text{total}} = \Gamma'_0 R' \tag{25}$$

with

$$R' = \sum_\alpha X_\alpha g_\alpha \sim 3.29 + 3.37 S_\gamma^2 + 3.25 S_\beta^2 + O\left(S_\beta^2, S_\gamma^2\right) \tag{26}$$

To obtain the final charged multilepton production cross sections from the $h\bar{h}$ pair decays ($h = b$ or t), there is need to compute probabilities $P_0^{(\alpha)}$, $P_1^{(\alpha)}$ and $P_2^{(\alpha)}$ for the final state in the decay of b to contain 0, 1, or 2 charged leptons, respectively; then probabilities B_0, B_1, and B_2 for the emission of 0, 1, or 2 charged leptons in b decays, to be followed by the probabilities $(B\bar{B})_n$ ($n = 0,1,2,3,4$) for charged multilepton emissions in the weak decays of a $b\bar{b}$ pair. Next, one computes probabilities $P_0'^{(\alpha)}$, $P_1'^{(\alpha)}, \ldots, P_5'^{(\alpha)}$, for the final state in the decay of t to contain $0,1,2,\ldots,$ or 5 charged leptons, respectively, for each channel α; then probabilities $T_0, T_1, \ldots, T_5$, for the emission of $0,1,2,3,4,$ or 5 charged leptons in t decays, to be followed by the computation of probabilities $(T\bar{T})_n$ ($n = 0,1,2,\ldots,10$) for charged multilepton emissions in the weak decays of a $t\bar{t}$ pair.

Assuming $Br(c \to l) \sim 0.2$, $Br(\tau \to l) \sim 0.34$, and using Table 1, we compute $P_0^{(\alpha)}$, $P_1^{(\alpha)}$, and $P_3^{(\alpha)}$, which are displayed in Table III.

Next, we compute B_0, B_1, and B_2 to obtain

$$B_0 = \sum_\alpha Br(b \to \alpha) \cdot P_0^{(\alpha)}$$

$$= \sum_\alpha \Gamma_b^\alpha P_0^{(\alpha)} / \Gamma_{\text{total}}^b = \sum_\alpha \Gamma_b^\alpha \cdot P_0^{(\alpha)} / \Gamma_0^b R \tag{27}$$

$$\sim \frac{1}{R}\left[1.48 S_\gamma^2 + 5.28 S_\beta^2 + O\left(S_\gamma^4, S_\beta^4\right)\right] \tag{28}$$

$$B_1 \sim \frac{1}{R}\left[1.92 S_\gamma^2 + 2.42 S_\beta^2 + O\left(S_\gamma^4, S_\beta^4\right)\right] \tag{29}$$

$$B_2 \sim \frac{1}{R}\left[0.18 S_\gamma^2 + O\left(S_\gamma^4, S_\beta^2\right)\right] \tag{30}$$

Then we compute the $(B\bar{B})_n$'s, $n = 0,1,2,3,4$:

$$(B\bar{B})_0 = \sum_\alpha Br(b \to \alpha) P_0^{(\alpha)} \cdot \sum_{\alpha'} Br(\bar{b} \to \alpha') P_0^{(\alpha')} \tag{31}$$

Table III. Probabilities $P_0^{(\alpha)}$, $P_1^{(\alpha)}$, $P_2^{(\alpha)}$

Channel α	$P_0^{(\alpha)}$	$P_1^{(\alpha)}$	$P_2^{(\alpha)}$
$b \to cl^- \bar{\nu}_l$	0	0.8	0.2
$\to c\tau^- \nu_\tau$	$Br(c \to l)_{\cap} B(\tau \to l)$ $= (0.8)(0.66) \sim 0.53$	$Br(c \to l)_{\cap} B(\tau \to l)$ $+ Br(c \to l)_{\cap} Br(\tau \to l)$ $= 0.40$	$Br(c \to l) Br(\tau \to l)$ ~ 0.07
$\to ul^- \bar{\nu}_l$	0	1.00	0
$\to u\tau^- \bar{\nu}_\tau$	0.66	0.34	0
$\to c\bar{u}d_c$	0.80	0.20	0
$\to c\bar{c}s_c$	0.64	0.32	0.04
$\to u\bar{u}d_c$	1.00	0	0
$\to u\bar{c}s_c$	0.80	0.20	0

If we take it that $P_n^{(\alpha)} = P_n^{(\alpha')}$, for $n = 0$, 1, 2 and $Br(b \to \alpha) = Br(\bar{b} \to \alpha')$, equation (31) gives the following:

$$(B\bar{B})_0 \equiv B_0 \bar{B}_0 \sim B_0^2 \tag{32}$$

$$(B\bar{B})_1 \equiv B_0 \bar{B}_1 + B_1 \bar{B}_0 \sim 2B_0 B_1 \tag{33}$$

$$(B\bar{B})_2 \sim 2B_0 B_2 + B_1^2 \tag{34}$$

$$(B\bar{B})_3 \sim 2B_1 B_2 \tag{35}$$

$$(B\bar{B})_4 \sim B_2^2 \tag{36}$$

Using the computed values of $P_0'^{(\alpha)}$, $P_1'^{(\alpha)}, \ldots, P_5'^{(\alpha)}$, displayed in Table IV, we next obtain T_n's ($n = 0, 1, 2, 3, 4, 5$):

$$T_0 = \sum_\alpha Br(t \to \alpha) P_0'^{(\alpha)} = \sum_\alpha X_\alpha g_\alpha P_0'^{(\alpha)} / R'$$

$$\sim \frac{1}{R'} \left[2.48B_0 - 3.38B_0 S_\gamma^2 - 3.84B_0 S_\beta^2 \right.$$

$$\left. + 2.69S_\gamma^2 + 2.69S_\beta^2 + 0.19B_0^2 S_\gamma^2 + 0.36S_\beta^2 B_0^2 + O\left(S_\gamma^4, S_\beta^4\right) \right] \tag{37}$$

Table IV. Probabilities $P_0'^{(\alpha)}, P_1'^{(\alpha)}, \ldots, P_5'^{(\alpha)}$

α	$P_0'^{(\alpha)}$	$P_1'^{(\alpha)}$	$P_2'^{(\alpha)}$	$P_3'^{(\alpha)}$	$P_4'^{(\alpha)}$	$P_5'^{(\alpha)}$
$t \to bl^+\nu_l$	0	B_0	B_1	B_2	0	0
$t \to b\tau_{\nu_\tau}^+$	$0.66B_0$	$0.66B_1+0.34B_0$	$0.34B+0.66B_2$	$0.34B_2$	0	0
$\to ql^+\nu_l$	0	1.00	0	0	0	0
$\to q\tau^+\nu_\tau$	0.66	0.34	0	0	0	0
$\to bu\bar{q}$	B_0	B_1	B_2	0	0	0
$\to bc\bar{q}$	$0.8B_0$	$0.2B_0+0.8B_1$	$0.2B_1+0.8B_2$	$0.2B_2$	0	0
$\to qu\bar{q}$	0	0	0	0	0	0
$\to qc\bar{q}$	0.80	0.20	0	0	0	0
$\to q\bar{b}c$	$0.8B_0$	$0.2B_0+0.8B_1$	$0.2B_1+0.8B_2$	$0.2B_2$	0	0
$\to q\bar{b}u$	B_0	B_1	B_2	0	0	0
$\to b\bar{b}c$	$0.8B_0$	$0.2B_0^2+1.6B_0B_1$	$0.4B_0B_1+1.6B_0B_2$	$2B_0B_2+1.6B_1B_2$	$0.8B_0^2$	$0.2B_2^2$
$\to b\bar{b}u$	B_0^2	$2B_0B_1$	$2B_0B_1+2B_1^2$	$2B_1B_2$	B_2^2	0

with

$$R' \sim 3.29+3.37S_\gamma^2+3.25S_\beta^2+O\left(S_\gamma^4, S_\beta^4\right) \tag{38}$$

$$T_1 \sim \frac{1}{R'}\left[0.8B_0+2.49B_1+\left(1.83-1.02B_0-3.38B_1+0.05B_0^2+0.38B_0B_1\right)S_\gamma^2\right.$$
$$\left.+\left(1.83-0.8B_0-3.84B_1+0.72B_0B_1\right)S_\beta^2+O\left(S_\gamma^4, S_\beta^4\right)\right] \tag{39}$$

$$T_2 \sim \frac{1}{R'}\left[0.22B_0+1.47B_1+1.66B_2\right.$$
$$+\left(0.31B_1-0.44B_0+0.96B_0B_1+0.38B_0B_2-2.95B_2\right)S_\gamma^2$$
$$\left.+\left(0.72B_0B_2-0.22B_0+0.72B_1^2-0.48B_1-2.5B_2\right)S_\beta^2\right] \tag{40}$$

$$T_3 \sim \frac{1}{R'}\left[B_2\left(0.80-1.02S_\gamma^2-0.80S_\beta^2\right)+0.48B_0B_2S_\gamma^2\right.$$
$$\left.+B_1B_2\left(0.38S_\gamma^2+0.72S_\beta^2\right)\right] \tag{41}$$

$$T_4 \sim \frac{1}{R'}\left(0.192B_2^2S_\gamma^2+0.36B_2^2S_\beta^2\right) \tag{42}$$

$$T_5 \sim \frac{1}{R'}\left(0.05B_2^2S_\gamma^2\right) \tag{43}$$

Finally, we compute probabilities $(T\bar{T})_n$, $(n=0,1,\ldots,10)$ for the emission of $0,1,2,\ldots,10$ charged multileptons in the weak decays of the $t\bar{t}$ pair:

Specifically, we obtain

$$(T\bar{T})_0 = \sum_{\alpha} Br(t \to \alpha) P_0^{\prime(\alpha)} \cdot \sum_{\alpha'} Br(\bar{t} \to \alpha') P_0'(\alpha') \tag{44}$$

If we take $P_r^{\prime(\alpha)} = P_r^{\prime(\alpha')}$, $r = 1,2,3,\ldots,5$ and $B_r(t \to \alpha) = Br(\bar{t} \to \alpha')$, equation (44) gives the following:

$$\begin{aligned}(T\bar{T})_0 &\equiv T_0\bar{T}_0 \sim T_0^2 \\ &= \frac{1}{R'}\left[B_0\left(2.49 - 3.17S_\gamma^2 - 3.59_\beta^2\right) + 2.7\left(S_\gamma^2 + S_\beta^2\right) + 0.36B_0^2S_\beta^2\right]\end{aligned} \tag{45}$$

$$\begin{aligned}&(T\bar{T})_1 \sim 2T_0T_1, \qquad (T\bar{T})_2 \sim 2T_0T_2 + T_1^2 \\ &(T\bar{T})_3 \sim 2T_3T_0 + 2T_2T_1, \qquad (T\bar{T})_4 \sim 2T_4T_0 + 2T_3T_1 + T_2^2 \\ &(T\bar{T})_5 \sim 2T_5T_0 + 2T_4T_1 + 2T_3T_2 \\ &(T\bar{T})_6 \sim 2T_5T_1 + 2T_4T_2 + T_3^2 \\ &(T\bar{T})_7 \sim 2T_5T_2 + 2T_4T_3 \\ &(T\bar{T})_8 \sim 2T_5T_3 + T_4^2 \\ &(T\bar{T})_9 \sim 2T_5T_3 + T_4^2 \\ &(T\bar{T})_{10} \sim T_5^2\end{aligned} \tag{46}$$

The charged multilepton production total cross sections from the production of $b\bar{b}$ and $t\bar{t}$ pairs in $\bar{p}p$ collisions and their weak decays are, respectively, given by

$$\sigma_n = (B\bar{B})_n \cdot \sigma(\bar{p}p \to b\bar{b}X), \qquad n = 0,1,2,3,4 \tag{47}$$

and

$$\sigma_n = (T\bar{T})_n \cdot \sigma(\bar{p}p \to t\bar{t}X), \qquad n = 0,1,2,3,\ldots,10 \tag{48}$$

4. NUMERICAL RESULTS

In order to obtain numerical results for the various cross sections, one has to prescribe quark and gluon distributions. Following Altarelli et al.

(Altarelli et al., 1976), one decomposes quark distributions as follows:

$$
\begin{aligned}
u(x,Q^2) &= u_v(x,Q^2)+\lambda(x,Q^2)\\
d(x,Q^2) &= d_v(x,Q^2)+\lambda(x,Q^2)\\
\bar{d}(x,Q^2) &= \bar{u}(x,Q^2)=\lambda(x,Q^2)=\bar{\lambda}(x,Q^2)\\
s(x,Q^2) &= 6\lambda(x,Q^2)\\
V_8(x,Q^2) &= u_v(x,Q^2)+d_v(x,Q^2)\\
V_3(x,Q^2) &= u_v(x,Q^2)-d_v(x,Q^2)
\end{aligned}
\tag{49}
$$

From the last two equations of (49), we obtain

$$
xu_v=\tfrac{1}{2}(xV_8+xV_3), \qquad xd_v=\tfrac{1}{2}(xV_8-xV_3) \tag{50}
$$

For the parton distributions, we use the parametrization of Buras and Gaemers (1978):

$$
xV_8=\frac{3}{B[\eta_1(\bar{s}),1+\eta_2(\bar{s})]}x^{\eta_1(\bar{s})}(1-x)^{\eta_2(\bar{s})} \tag{51}
$$

$$
xV_8-xV_3=\frac{2}{B[\eta_3(\bar{s}),1+\eta_4(\bar{s})]}x^{\eta_3(\bar{s})}(1-x)^{\eta_4(\bar{s})} \tag{52}
$$

with

$$
\begin{aligned}
\eta_1(\bar{s}) &= 0.70-1.1G\bar{s}\\
\eta_2(\bar{s}) &= 2.60+5G\bar{s}\\
\eta_3(\bar{s}) &= 0.85-1.5G\bar{s}\\
\eta_4(\bar{s}) &= 3.35+5.1G\bar{s}
\end{aligned}
\tag{53}
$$

and $G \sim 4/21$, for six flavors of quarks (Politzer, 1974; Gross and Wilczek, 1974; Georgi and Politzer, 1974; Balin, et al., 1974).

One easily deduces the following:

$$
xu_v(x,Q^2)=\frac{3x^{\eta_1}(1-x)^{\eta_2}}{B(\eta_1,1+\eta_2)}-\frac{x^{\eta_3}(1-x)^{\eta_4}}{B(\eta_3,1+\eta_4)} \tag{54}
$$

$$
xd_v(x,Q^2)=\frac{x^{\eta_3}(1-x)^{\eta_4}}{B(\eta_3,1+\eta_4)} \tag{55}
$$

with

$$\eta_1(\bar{s}) \sim 0.70 - 0.21\bar{s}$$

$$\eta_2(\bar{s}) \sim 2.60 + 0.95\bar{s}$$

$$\eta_3(\bar{s}) \sim 0.85 - 0.29\bar{s}$$

$$\eta_4(\bar{s}) \sim 3.35 + 0.97\bar{s} \tag{56}$$

and

$$\bar{s} = \ln\left[\frac{\ln(Q^2/\Lambda^2)}{\ln(Q_0^2/\lambda^2)}\right] \tag{57}$$

where $\Lambda \sim 0.5$, $Q_0^2 \sim 1.8$ GeV.

For $Q^2 = 4m_t^2$, one obtains $\bar{s} \sim 0.61$, so that

$$\eta_1 \sim 0.57, \qquad \eta_2 \sim 3.18, \qquad \eta_3 \sim 0.67, \qquad \eta_4 \sim 3.94$$

If we take the mass of the top as 14 GeV (Georgi and Nanopoulos, 1979), then equations (54) and (55) modify to

$$xu_v^p(x,Q^2)|_{Q^2=4m_t^2\sim 784} \simeq \frac{3x^{0.57}(1-x)^{3.18}}{B(0.58,4.18)} - \frac{x^{0.67}(1-x)^{3.94}}{B(0.67,4.94)} \tag{58}$$

and

$$xd_v^p(x,Q^2)|_{Q^2=784} \sim \frac{x^{0.67}(1-x)^{3.94}}{B(0.67,4.94)} \tag{59}$$

For the gluon distribution, we adopt the structure

$$xG(x,\bar{s}) = A_G(\bar{s})(1-x)^{\eta_G(\bar{s})} \tag{60}$$

in the presence of ASFT effects, with $A_G(\bar{s}) \sim 7.94$ at $\bar{s} \sim 0.6$, i.e., at $Q^2 \sim 4m_t^2|_{m_t\sim 14} \approx 784$ GeV, $\eta_G(\bar{s}) = 16.14$ also at $Q^2 \sim 784$ GeV. Hence, equation (60) gives

$$xG^p(x,Q^2) \sim 7.4(1-x)^{16.4} \tag{61}$$

We also use the following parameters: $m_\alpha = 0.35$ GeV,

$$\alpha_s(Q^2)|_{Q^2=4m_t^2\sim 784} \approx 0.23, \qquad \Lambda \sim 0.5$$

for six flavors of quarks.

Table V. Total Cross Sections for the Production of $b\bar{b}$ Pairs in $\bar{p}p$ Collisions as a Function of $\sqrt{S}$

$\sqrt{S}$ (GeV)	$\sigma(\bar{p}p \to b\bar{b}X)$ (cm^2)
20	1.3×10^{-34}
30	1.7×10^{-33}
40	7.7×10^{-32}
60	1.7×10^{-32}
100	4.6×10^{-32}
200	2.8×10^{-31}
300	1.3×10^{-30}
400	1.7×10^{-30}
500	2.8×10^{-30}
600	4.6×10^{-30}
700	4.7×10^{-30}
800	10^{-29}

Table VI. Total Cross Sections for the Production of $t\bar{t}$ Pairs in $\bar{p}p$ Collisions at $\sqrt{S} = 62.5$ and 800 GeV

$\sqrt{S}$ (GeV)	$\sigma(\bar{p}p \to t\bar{t}X)$ (cm^2)
62.5	9.5×10^{-35}
800	1.5×10^{-3}

Table VII. Probabilities $(B\bar{B})_n$ $(n = 0,1,2,3,4)$ Evaluated for the Pairs (S_γ, β) of the Quark Mixing Angles

(S_γ, β)	$(B\bar{B})_0$	$(B\bar{B})_1$	$(B\bar{B})_2$	$(B\bar{B})_3$	$(B\bar{B})_4$
(0,0.12)	0.38	0.44	0.012	0	0
(−0,133,0)	0.29	0.76	0.56	0.09	0.004
(−0.133,0.08)	0.37	0.62	0.297	0.031	0.0009
(−0.4,0)	0.29	0.51	0.29	0.06	0.004
(−0.133,0.04)	0.31	0.69	0.44	0.062	0.0025
(−0.266,0.08)	0.33	0.72	0.458	0.0.067	0.0028
(−0.133,0.12)	0.41	0.56	0.217	0.0175	0.0004
(−0.266,0.04)	0.29	0.72	0.46	0.0.018	0.00019
(−0.266,0.12)	0.35	0.66	0.36	0.045	0.0016

Table VIII. Probabilities $(T\bar{T})_n$ $(n = 0, 1, 2, \ldots, 10)$ Evaluated for Assigned Numerical Values of the Pairs (S_γ, β) of the Quark Mixing Angles

(S_γ, β)	$(T\bar{T})_0$	$(T\bar{T})_1$	$(T\bar{T})_2$	$(T\bar{T})_3$	$(T\bar{T})_4$	$(T\bar{T})_5$	$(T\bar{T})_6$	$(T\bar{T})_7$	$(T\bar{T})_8$	$(T\bar{T})_9$	$(T\bar{T})_{10}$
(0,0.12)	0.27	0.42	0.36	0.15	0.04	0	0	0	0	0	0
(0,0.08)	0.27	0.42	0.36	0.15	0.04	0	0	0	0	0	0
(0,0.04)	0.27	0.43	0.36	0.152	0.035	0	0	0	0	0	0
(−0.133,0)	0.17	0.52	0.72	0.49	0.16	0.012	2.6×10^{-4}	9.4×10^{-7}	3.5×10^{-8}	9.6×10^{-12}	1.2×10^{-12}
(−0.4,0)	0.15	0.41	0.54	0.36	0.122	0.008	2.6×10^{-4}	6.3×10^{-6}	2.11×10^{-8}	5.6×10^{-10}	7.1×10^{-11}
(0,0.12) (0,0,08) (0,0.04)	0.27	0.42	0.36	0.15	0.034	0	0	0	0	0	0
(−0.133,0)	0.17	0.52	0.72	0.49	0.16	1.2×10^{-2}	2.6×10^{-4}	9.4×10^{-7}	3.5×10^{-8}	9.68×10^{-12}	1.2×10^{-12}
(−0.133,0.08)	2.07×10^{-1}	4.7×10^{-2}	5.2×10^{-1}	2.6×10^{-2}	1.5×10^{-2}	4.2×10^{-4}	6×10^{-5}	1.5×10^{-6}	4×10^{-8}	9.6×10^{-12}	7.1×10^{-12}
(−0.133,0.04)	0.18	0.49	0.62	0.39	0.112	3.4×10^{-3}	2.4×10^{-5}	8.2×10^{-8}	1.09×10^{-9}	10^{-9}	1.9×10^{-14}
(−0.133,0.12)	0.014	0.08	0.15	0.123	0.04	6.7×10^{-4}	1.3×10^{-5}	2.5×10^{-8}	4.5×10^{-10}	2.3×10^{-14}	3.9×10^{-15}
(−0.266,0)	0.16	0.48	0.64	0.44	0.145	0.01	2.16×10^{-4}	8.2×10^{-7}	1.2×10^{-7}	1.4×10^{-10}	1.7×10^{-11}
(−0.266,0.04)	0.16	0.47	0.62	0.42	0.14	9.3×10^{-3}	1.9×10^{-4}	2.9×10^{-6}	9.7×10^{-8}	1.1×10^{-10}	1.3×10^{-11}
(−0.266,0.08)	0.17	0.46	0.57	0.36	0.11	7.1×10^{-3}	1.3×10^{-4}	1.9×10^{-6}	5.8×10^{-8}	6.4×10^{-11}	6.8×10^{-12}
(−0.266,0.12)	0.18	0.44	0.51	0.29	0.09	5×10^{-3}	8.3×10^{-5}	1.1×10^{-6}	2.9×10^{-8}	3×10^{-11}	2.7×10^{-12}

Table IX. Charged Multilepton Production Cross Sections from the Production of $b\bar{b}$ Pairs in $\bar{p}p$ Collision and Subsequent Weak Decays: $(S_\gamma, \beta) = (0, 0.12)$

$\sqrt{S}$ (GeV)	σ_0 (cm^2)	σ_1 (cm^2)	σ_2 (cm^2)	σ_3 (cm^2)	σ_4 (cm^2)
20	6.2×10^{-35}	5.7×10^{-35}	1.3×10^{-35}	0	0
60	8.1×10^{-35}	7.5×10^{-33}	1.7×10^{-33}	0	0
100	2.2×10^{-32}	2×10^{-32}	4.7×10^{-33}	0	0
400	8.1×10^{-31}	7.5×10^{-31}	1.7×10^{-31}	0	0
800	4.76×10^{-30}	4.4×10^{-30}	10^{-30}	0	0

Table X. Charged Multilepton Production Cross Sections from the Production of $b\bar{b}$ Pairs in $\bar{p}p$ Collision and Subsequent Weak Decays: $(S_\gamma, \beta) = (-0.133, 0)$

$\sqrt{S}$ (GeV)	σ_0 (cm^2)	σ_1 (cm^2)	σ_2 (cm^2)	σ_3 (cm^2)	σ_4 (cm^2)
20	3.8×10^{-35}	9.9×10^{-35}	7.3×10^{-35}	1.2×10^{-35}	5.2×10^{-38}
60	4.9×10^{-33}	1.3×10^{-32}	9.5×10^{-35}	1.5×10^{-33}	6.8×10^{-36}
100	1.3×10^{-32}	3.5×10^{-32}	2.6×10^{-32}	4.2×10^{-33}	1.8×10^{-34}
400	4.9×10^{-31}	1.3×10^{-30}	9.5×10^{-31}	1.5×10^{-31}	6.8×10^{-33}
800	2.9×10^{-30}	7.6×10^{-30}	5.6×10^{-30}	9×10^{-31}	4×10^{-32}

Table XI. Charged Multilepton Production Cross Sections from the Production of $b\bar{b}$ Pairs in $\bar{p}p$ Collision and Subsequent Weak Decays: $(S_\gamma, \beta) \equiv (-0.4, 0)$

$\sqrt{S}$ (GeV)	σ_0 (cm^2)	σ_1 (cm^2)	σ_2 (cm^2)	σ_3 (cm^2)	σ_4 (cm^2)
20	3.8×10^{-35}	6.6×10^{-35}	3.8×10^{-35}	7.8×10^{-36}	5.2×10^{-37}
60	4.9×10^{-33}	8.7×10^{-33}	4.9×10^{-33}	1.1×10^{-33}	6.8×10^{-35}
100	1.3×10^{-32}	2.3×10^{-32}	1.3×10^{-32}	2.8×10^{-33}	1.8×10^{-34}
400	4.9×10^{-31}	8.7×10^{-31}	4.9×10^{-31}	1.1×10^{-31}	6.8×10^{-33}
800	2.9×10^{-30}	5.1×10^{-30}	2.9×10^{-30}	6×10^{-31}	4×10^{-32}

Table XII. Charged Multilepton Production Cross Sections from the Production of $b\bar{b}$ Pairs in $\bar{p}p$ Collision and Subsequent Weak Decays: $(S_\gamma, \beta) \equiv (-0.133, 0.08)$

$\sqrt{S}$ (GeV)	σ_0 (cm^2)	σ_1 (cm^2)	σ_2 (cm^2)	σ_3 (cm^2)	σ_4 (cm^2)
20	4.8×10^{-35}	8.1×10^{-35}	3.9×10^{-35}	4×10^{-36}	1.2×10^{-37}
60	6.3×10^{-33}	1.1×10^{-32}	5.1×10^{-33}	5.3×10^{-34}	1.5×10^{-35}
100	1.7×10^{-32}	2.9×10^{-32}	1.4×10^{-32}	1.4×10^{-33}	4.2×10^{-35}
400	6.3×10^{-31}	1.1×10^{-30}	5×10^{-31}	5.3×10^{-32}	1.5×10^{-33}
800	3.7×10^{-30}	6.2×10^{-30}	2.9×10^{-30}	3.1×10^{-31}	9×10^{-33}

Table XIII. Charged Multilepton Production Cross Sections from the Production of $b\bar{b}$ Pairs in $\bar{p}p$ Collision and Subsequent Weak Decays: $(S_\gamma, \beta) \equiv (-0.133, 0.04)$

$\sqrt{S}$ (GeV)	σ_0 (cm^2)	σ_1 (cm^2)	σ_2 (cm^2)	σ_3 (cm^2)	σ_4 (cm^2)
20	4×10^{-35}	8.9×10^{-35}	5.7×10^{-35}	8.1×10^{-36}	3.3×10^{-37}
60	5.3×10^{-33}	1.2×10^{-32}	7.5×10^{-33}	1.1×10^{-33}	4.3×10^{-35}
100	1.4×10^{-32}	3.2×10^{-32}	2×10^{-32}	2.8×10^{-33}	1.2×10^{-34}
400	5.3×10^{-31}	1.2×10^{-30}	7.5×10^{-31}	1.1×10^{-31}	4.3×10^{-33}
800	3.1×10^{-30}	6.9×10^{-30}	4.4×10^{-30}	6.2×10^{-31}	2.5×10^{-32}

Table XIV. Charged Multilepton Production Cross Sections from the Production of $b\bar{b}$ Pairs in $\bar{p}p$ Collision and Subsequent Weak Decays: $(S_\gamma, \beta) \equiv (-0.266, 0.08)$

$\sqrt{S}$ (GeV)	σ_0 (cm^2)	σ_1 (cm^2)	σ_2 (cm^2)	σ_3 (cm^2)	σ_4 (cm^2)
20	4.3×10^{-35}	9.4×10^{-35}	5.9×10^{-35}	8.7×10^{-36}	3.6×10^{-37}
60	5.6×10^{-33}	1.2×10^{-32}	7.8×10^{-33}	1.1×10^{-33}	4.8×10^{-35}
100	1.5×10^{-32}	3.3×10^{-32}	2.1×10^{-32}	3.1×10^{-33}	1.3×10^{-34}
400	5.6×10^{-31}	1.2×10^{-30}	7.8×10^{-31}	1.1×10^{-31}	4.8×10^{-33}
800	3.3×10^{-30}	7.2×10^{-30}	4.6×10^{-30}	6.7×10^{-31}	2.8×10^{-32}

Table XV. Charged Multilepton Production Cross Sections from the Production of $b\bar{b}$ Pairs in $\bar{p}p$ Collision and Subsequent Weak Decays: $(S_\gamma, \beta) = (-0.133, 0.12)$

$\sqrt{S}$ (GeV)	σ_0 (cm^2)	σ_1 (cm^2)	σ_2 (cm^2)	σ_3 (cm^2)	σ_4 (cm^2)
20	5.3×10^{-35}	7.3×10^{-35}	2.8×10^{-35}	2.3×10^{-36}	5.2×10^{-38}
60	6.9×10^{-33}	9.5×10^{-33}	3.7×10^{-33}	2.9×10^{-34}	6.8×10^{-36}
100	1.9×10^{-32}	2.6×10^{-32}	9.9×10^{-33}	8.1×10^{-34}	1.8×10^{-35}
400	6.9×10^{-31}	9.5×10^{-31}	3.7×10^{-31}	2.9×10^{-32}	6.8×10^{-34}
800	4.1×10^{-30}	5.6×10^{-30}	2.2×10^{-30}	$1.8\times10^{-31}4\times10^{-33}$	

Table XVI. Charged Multilepton Production Cross Sections from the Production of $b\bar{b}$ Pairs in $\bar{p}p$ Collision and Subsequent Weak Decays: $(S_\gamma, \beta) = (-0.266, 0.04)$

$\sqrt{S}$ (GeV)	σ_0 (cm^2)	σ_1 (cm^2)	σ_2 (cm^2)	σ_3 (cm^2)	σ_4 (cm^2)
20	3.8×10^{-35}	9.4×10^{-35}	5.9×10^{-35}	2.3×10^{-36}	2.5×10^{-38}
60	4.9×10^{-33}	1.2×10^{-32}	7.8×10^{-33}	3.1×10^{-34}	3.2×10^{-36}
100	1.3×10^{-32}	3.3×10^{-32}	2.1×10^{-32}	8.3×10^{-34}	8.7×10^{-36}
400	4.9×10^{-31}	1.2×10^{-30}	7.8×10^{-31}	3.1×10^{-32}	3.2×10^{-34}
800	2.9×10^{-30}	7.2×10^{-30}	4.6×10^{-30}	1.8×10^{-31}	1.9×10^{-33}

Table XVII. Charged Multilepton Production Cross Sections from the Production of $b\bar{b}$ Pairs in $\bar{p}p$ Collision and Subsequent Weak Decays: $(S_\gamma, \beta) \equiv (-0.266, 0.12)$

$\sqrt{S}$ (GeV)	σ_0 (cm^2)	σ_1 (cm^2)	σ_2 (cm^2)	σ_3 (cm^2)	σ_4 (cm^2)
20	4.6×10^{-35}	8.6×10^{-35}	4.7×10^{-35}	5.9×10^{-36}	2.1×10^{-37}
60	5.9×10^{-33}	1.1×10^{-32}	6.1×10^{-33}	7.7×10^{-34}	2.7×10^{-35}
100	1.6×10^{-32}	3×10^{-32}	1.7×10^{-32}	2.1×10^{-33}	7.4×10^{-35}
400	5.9×10^{-31}	1.1×10^{-30}	6.1×10^{-31}	7.7×10^{-32}	2.7×10^{-33}
800	3.5×10^{-30}	6.6×10^{-30}	3.6×10^{-30}	4.5×10^{-31}	1.6×10^{-32}

Table XVIII. Charged Multilepton Production Cross Sections from $t\bar{t}$ Pair Production and Subsequent Weak Decays: $(S_\gamma, \beta) = (0, 0.12)$

$\sqrt{S}$	σ_0	σ_{s1}	σ_2	σ_3	σ_4	σ_5	σ_6	σ_7	σ_8	σ_9	σ_{10}
62.5	2.6×10^{-35}	3.9×10^{-35}	3.4×10^{-35}	1.4×10^{-35}	3.8×10^{-36}	0	0	0	0	0	0
800	4.1×10^{-32}	6.3×10^{-32}	5.4×20^{-31}	2.3×10^{-32}	6×10^{-33}	0	0	0	0	0	0

Table XIX. Charged Multilepton Production Cross Sections from $t\bar{t}$ Pair Production and Subsequent Weak Decays: $(S_\gamma, \beta) = (-0.133, 0)$

$\sqrt{S}$	σ_0	σ_1	σ_2	σ_3	σ_4	σ_5	σ_6	σ_7	σ_8	σ_9	σ_{10}
62.5	1.6×10^{-35}	4.9×10^{-35}	4.8×10^{-35}	4.6×10^{-35}	1.5×10^{-35}	1.4×10^{-36}	2.5×10^{-38}	8.9×10^{-41}	3.3×10^{-42}	9.1×10^{-44}	1.1×10^{-44}
800	2.6×10^{-32}	7.8×10^{-32}	1.1×10^{-31}	7.4×10^{-32}	2.4×10^{-32}	1.8×10^{-33}	3.9×10^{-35}	1.4×10^{-37}	5.3×10^{-39}	1.4×10^{-42}	1.8×10^{-43}

Table XX. Charged Multilepton Production Cross Sections from $t\bar{t}$ Pair Production and Subsequent Weak Decays: $(S_\gamma, \beta) = (-0.4, 0)$

$\sqrt{S}$	σ_0	σ_1	σ_2	σ_3	σ_4	σ_5	σ_6	σ_7	σ_8	σ_9	σ_{10}
62.5	1.4×10^{-35}	3.9×10^{-35}	5.1×10^{-35}	3.4×10^{-35}	1.2×10^{-35}	7.6×10^{-37}	2.5×10^{-38}	5.9×10^{-38}	2×10^{-42}	5.3×10^{-44}	6.7×10^{-45}
800	2.2×10^{-32}	6.1×10^{-32}	8.1×10^{-32}	5.4×10^{-32}	1.8×10^{-32}	1.2×10^{-33}	3.9×10^{35}	3.2×10^{-39}	3.2×10^{-39}	8.4×10^{-41}	1.1×10^{-41}

Table XXI. Charged Multilepton Production Cross Sections from $t\bar{t}$ Pair Production and Subsequent Weak Decays: $(S_\gamma, \beta) = (-0.133, 0.08)$

$\sqrt{S}$	σ_0	σ_1	σ_2	σ_3	σ_4	σ_5	σ_6	σ_7	σ_8	σ_9	σ_{10}
62.5	1.9×10^{-35}	4.5×10^{-35}	4.9×10^{-35}	2.5×10^{-36}	1.4×10^{-38}	5.7×10^{-39}	1.4×10^{-40}	1.4×10^{-40}	3.8×10^{-42}	$9.\times10^{-46}$	6.7×10^{-46}
800	3.1×10^{-32}	7.1×10^{-32}	7.8×10^{-31}	3.9×10^{-33}	6.3×10^{-35}	9×10^{-36}	9×10^{-36}	2.3×10^{-37}	6×10^{-39}	1.4×10^{-42}	1.1×10^{-42}

Table XXII. Charged Multilepton Production Cross Sections from $t\bar{t}$ Pair Production and Subsequent Weak Decays: $(S_\gamma, \beta) = (-0.133, 0.08)$

$\sqrt{S}$	σ_0	σ_1	σ_2	σ_3	σ_4	σ_5	σ_6	σ_7	σ_8	σ_9	σ_{10}
62.5	1.9×10^{-35}	4.5×10^{-35}	4.9×10^{-35}	2.5×10^{-36}	1.4×10^{-36}	3.9×10^{-38}	5.7×10^{-39}	1.4×10^{-40}	3.8×10^{-42}	9.1×10^{-46}	6.7×10^{-46}
800	3.1×10^{-32}	7.1×10^{-32}	7.8×10^{-31}	3.9×10^{-32}	2.3×10^{-33}	6.3×10^{-35}	9×10^{-36}	2.3×10^{-37}	6×10^{-39}	1.4×10^{-42}	1.1×10^{-42}

Table XXIII. Charged Multilepton Production Cross Sections from $t\bar{t}$ Pair Production and Subsequent Weak Decays: $(S_\gamma, \beta) = (-0.133, 0.04)$

$\sqrt{S}$	σ_0	σ_1	σ_2	σ_3	σ_4	σ_5	σ_6	σ_7	σ_8	σ_9	σ_{10}
62.5	1.7×10^{-35}	4.7×10^{-35}	5.9×10^{-35}	3.7×10^{-35}	1.1×10^{-35}	3.2×10^{-37}	2.3×10^{-39}	7.8×10^{-42}	1.1×10^{-43}	9.5×10^{-44}	1.8×10^{-48}
800	2.7×10^{-32}	7.4×10^{-32}	9.3×10^{-32}	5.9×10^{-32}	1.7×10^{-32}	5.1×10^{-34}	3.6×10^{-36}	1.2×10^{-38}	1.6×10^{-40}	1.5×10^{-40}	2.9×10^{-45}

Table XXIV. Charged Multilepton Production Cross Sections from $t\bar{t}$ Pair Production and Subsequent Weak Decays: $(S_\gamma, \beta) = (-0.266, 0.08)$

$\sqrt{S}$	σ_0	σ_1	σ_2	σ_3	σ_4	σ_5	σ_6	σ_7	σ_8	σ_9	σ_{10}
62.5	1.6×10^{-35}	4.4×10^{-35}	5.4×10^{-35}	3.4×10^{-35}	1.1×10^{-35}	6.7×10^{-37}	1.2×10^{-38}	1.8×10^{-40}	5.5×10^{-42}	6.1×10^{-45}	6.5×10^{-46}
800	2.6×10^{-32}	6.9×10^{-32}	8.6×10^{-32}	5.4×10^{-32}	1.7×10^{-32}	1.1×10^{-33}	1.9×10^{-35}	2.9×10^{-37}	8.7×10^{-39}	9.6×10^{-42}	10^{-42}

Table XXV. Charged Multilepton Production Cross Sections from $t\bar{t}$ Pair Production and Subsequent Weak Decays: $(-0.133, 0.12)$

$\sqrt{S}$	σ_0	σ_1	σ_2	σ_3	σ_4	σ_5	σ_6	σ_7	σ_8	σ_9	σ_{10}
62.5	1.3×10^{-36}	7.6×10^{-36}	1.4×10^{-35}	1.2×10^{-35}	3.8×10^{-36}	6.4×10^{-38}	1.2×10^{-39}	2.4×10^{-42}	4.3×10^{-44}	2.2×10^{-48}	3.7×10^{-49}
800	2.1×10^{-33}	1.2×10^{-32}	2.3×10^{-32}	1.8×10^{-32}	6×10^{-32}	10^{-35}	1.9×10^{-36}	3.8×10^{-39}	6.8×10^{-41}	3.5×10^{-45}	5.9×10^{-46}

Table XXVI. Charged Multilepton Production Cross Sections from $t\bar{t}$ Pair Production and Subsequent Weak Decays: $(S_\gamma, \beta) = (-0.266, 0.04)$

$\sqrt{S}$	σ_0	σ_1	σ_2	σ_3	σ_4	σ_5	σ_6	σ_7	σ_8	σ_9	σ_{10}
62.5	1.5×10^{-35}	4.5×10^{-35}	5.9×10^{-32}	3.9×10^{-35}	1.3×10^{-35}	8.8×10^{-37}	1.8×10^{-38}	2.8×10^{-40}	9.2×10^{-42}	1.1×10^{-44}	1.2×10^{-45}
800	2.4×10^{-32}	7.1×10^{-32}	9.3×10^{-32}	6.3×10^{-32}	2.1×10^{-32}	1.4×10^{-33}	2.9×10^{-32}	4.4×10^{-37}	1.5×10^{-38}	1.7×10^{-41}	1.9×10^{-42}

Table XXVII. Charged Multilepton Production Cross Sections from $t\bar{t}$ Pair Production and Subsequent Weak Decays: $(S_\gamma, \beta) = (-0.266, 0)$

$\sqrt{S}$	σ_0	σ_1	σ_2	σ_3	σ_4	σ_5	σ_6	σ_7	σ_8	σ_9	σ_{10}
62.5	1.5×10^{-35}	4.6×10^{-35}	6.1×10^{-35}	4.2×10^{-35}	1.4×10^{-35}	9.5×10^{-37}	2.1×10^{-38}	7.8×10^{-41}	1.1×10^{-41}	1.3×10^{-44}	1.6×10^{-45}
800	2.4×10^{-32}	7.2×10^{-32}	9.6×10^{-32}	6.6×10^{-32}	2.2×10^{-32}	1.5×10^{-33}	3.2×10^{-35}	1.2×10^{-37}	1.8×10^{-38}	2.1×10^{-41}	2.6×10^{-41}

Table XXVIII. Charged Multilepton Production Cross Sections from $t\bar{t}$ Pair Production and Subsequent Weak Decays: $(S_\gamma, \beta) = (-0.266, 0.12)$

$\sqrt{S}$	σ_0	σ_1	σ_2	σ_3	σ_4	σ_5	σ_6	σ_7	σ_8	σ_9	σ_{10}
62.5	1.7×10^{-35}	4.2×10^{-35}	4.8×10^{-35}	2.8×10^{-35}	8.6×10^{-36}	4.8×10^{-37}	7.9×10^{-39}	1.1×10^{-40}	2.8×10^{-42}	2.9×10^{-45}	2.6×10^{-46}
800	2.7×10^{-32}	6.6×10^{-32}	7.7×10^{-32}	4.4×10^{-32}	1.4×10^{-32}	7.5×10^{-34}	1.3×10^{-35}	1.7×10^{-37}	4.4×10^{-39}	4.5×10^{-42}	4.1×10^{-43}

For $Q^2 = 4m_b^2 \sim 117$ GeV, using $m_b \sim 5.4$ GeV, $\bar{s} = 0.5$, so that

$$xu_v^p(x,Q^2) \sim \frac{3x^{0.6}(1-x)^{3.1}}{B(0.6,4.1)} \frac{x^{0.7}(1-x)^{3.8}}{B(0.7,4.8)} \tag{62}$$

$$xd_v^p(x,Q^2) \sim \frac{x^{0.7}(1-x)^{3.8}}{B(0.7,4.8)} \tag{63}$$

$$xG^p(x,Q^2) \sim 8(1-x)^{16} \tag{64}$$

Substituting into equations (18), using equations (12) and (17′), we obtain the total cross sections $\sigma(\bar{p}p \to b\bar{b}X)$, for $\sqrt{s} \sim 20-800$ GeV and $\alpha_s^2(Q^2) \sim 0.30$, and $\sigma(\bar{p}p \to t\bar{t}X)$, for $\sqrt{s} \sim 62.5$ and 800 GeV. These are displayed in Tables V and VI, respectively.

Probabilities $(B\bar{B})_m$ $(m = 0,1,2,3,4)$ and $(T\bar{T})_n$ $(n = 0,1,2,\ldots,10)$, for arbitrarily chosen combinations (S_γ, β) of quark mixing angles, are displayed in Tables VII and VIII, respectively.

Charged multilepton total cross sections from the production of $b\bar{b}$, $t\bar{t}$ pairs in $\bar{p}p$ interactions, and their weak semileptonic and cascade decays are displayed in Tables IX–XXVIII.

5. SUMMARY

We have computed total cross sections for the production of $b\bar{b}$ and $t\bar{t}$ pairs in $\bar{p}p$ interactions as functions of $\sqrt{s}$, the $\bar{p}p$ center-of-mass energy. We have also obtained probabilities $(BB)_n$ $(n = 0,1,2,3,4)$ and $(T\bar{T})_n$ $(n = 0,1,2,\ldots,10)$ for the emission of charged multileptons from the weak and cascade decays of the $b\bar{b}$ and $t\bar{t}$ pairs. These probabilities are evaluated for arbitrarily assigned numerical values of pairs of the quark mixing angles, (s_γ, β). Also, charged multilepton production cross sections, σ_{n_b} $(n = 0,1,2,3,4)$ and σ_n $(n = 0,1,\ldots,10)$ from the production of $b\bar{b}$ and $t\bar{t}$ pairs, respectively, in $\bar{p}p$ collisions and their subsequent weak decays, are evaluated for the same combinations of pairs of the quark mixing angles, as in the above, and for present and projected experimental values of $\sqrt{s}$.

One observes, in our calculations, that the cross sections for the associated production of b and t in proton beams are more or less on the same footing with those for the production of charged multileptons arising from the weak decays of the pairs. The implication of this is that any charged multilepton signals that could be observed in proton beams would first have to result from the decays of the $b\bar{b}$ pairs rather than those of the $t\bar{t}$

pairs, and for that matter, a maximum of four charged leptons, as this is the number that is allowed by the bounds of the quark mixing angles used. The calculations also indicate that from the point of view of experimental searches for heavy flavored states in hadronic collisions, with particular interest in the bottom and top states, use of highest possible beam energies should be a major consideration as the production cross section of these states rise with increasing $\sqrt{s}$. Finally, one concludes, in the same vein, that on the basis of the associated production cross sections for b and t, which are more or less on the same footing with those for the production of charged multileptons resulting from the weak decays of their respective pairs, use of charged multilepton signals in a search for the bottom and top flavors or states, appears to be a new input, and the more intense the proton beams, the greater the chances of discovering these flavors or states in the beams.

As regards the magnitudes of the charged multilepton cross sections which we have computed, a general trend they exhibit is that these cross sections rise with increasing $\sqrt{s}$. The mixing angles γ and β have a sizeable effect on the cross sections. While certain combinations of pairs of these angles, within the allowed bounds, completely suppress the production of charged multileptons above charged tetraleptons, from the $t\bar{t}$ decays and dileptons from the $b\bar{b}$, some other pairs of the mixing angles give rise to the entire spectra of these charged multileptons; that is, from zero to four, in the case of the $b\bar{b}$ decays, and from zero to ten, in the case of the $t\bar{t}$ decays. For all the values of pairs of the mixing angles used, charged single-lepton production arising from the production and decay of the $b\bar{b}$ pairs has the highest incidence, theoretically, of course, followed by the dileptons. On the other hand, in the case of the $t\bar{t}$ pairs, charged dilepton production has the highest incidence. Thus it appears that the effect of the mixing angles of the quarks on the multilepton production cross sections is significant. It is hoped that when precise charged multilepton signals show up in future experimental searches for heavy quark flavors, they can help to discriminate the bounds and the magnitudes of the quark mixing angles to be used in our type of model.

REFERENCES

Altarelli, G., Petronzio, R., and Parisi, G. (1976). *Physical Review Letters*, **37**, 1313.
Balin, D., Love, A., and Nanopoulos, D. (1974). *Nuovo Cimento Letters*, **9**, 50.
Buras, A. J., and Gaemers, K. J. F. (1978). *Nuclear Physics B*, **132**, 249.
Cabibbo, N., and Maiani, L. (1979). Preprint CERN-TH-2726.

Gaillard, M. K., and Maiani, L. (1979). In Quarks and Leptons, Proc. of the 1979 Cargèse Summer School.

Georgi, H., and Politizer, H. D. (1974). *Physical Review D*, **9**, 416.

Maiani, L. (1977). Proc. of the 1977 Int. Symp. on Lepton and Photon Interactions at High Energies, Hamburg, edited by F. Gutbrod.

Politzer, H. D. (1974). *Physics Letters* **C14**, 129; Gross, D. and Wilczek, F. (1975). *Physical Review D*, **9**, 980, 3633.